Role of Quantum Coherence in Chromophoric Energy Transport

The Harvard community has made this article openly available. Please share how this access benefits you. Your story matters

Citation	Rebentros, Patrick, Masoud Mohseni, and Alán Aspuru-Guzik. 2009. Role of quantum coherence in chromophoric energy transport. Journal of Physical Chemistry B 113(29): 9942–9947.
Published Version	doi:10.1021/jp901724d
Citable link	http://nrs.harvard.edu/urn-3:HUL.InstRepos:4646384
Terms of Use	This article was downloaded from Harvard University's DASH repository, and is made available under the terms and conditions applicable to Open Access Policy Articles, as set forth at http://nrs.harvard.edu/urn-3:HUL.InstRepos:dash.current.terms-of-use#OAP

Role of quantum coherence in chromophoric energy transport

Patrick Rebentrost,[1] Masoud Mohseni,[1] and Alán Aspuru-Guzik[1]

[1]*Department of Chemistry and Chemical Biology, Harvard University, 12 Oxford St., Cambridge, MA 02138*
(Dated: February 4, 2009)

The role of quantum coherence and the environment in the dynamics of excitation energy transfer is not fully understood. In this work, we introduce the concept of dynamical contributions of various physical processes to the energy transfer efficiency. We develop two complementary approaches, based on a Green's function method and energy transfer susceptibilities, and quantify the importance of the Hamiltonian evolution, phonon-induced decoherence, and spatial relaxation pathways. We investigate the Fenna-Matthews-Olson protein complex, where we find a contribution of coherent dynamics of about 10% and of relaxation of 80%.

I. INTRODUCTION

Exciton transfer among chlorophyll molecules is the energy transport mechanism of the initial step of the photosynthetic process. Light is captured by an antenna complex and the exciton is subsequently transferred to a reaction center where bio-chemical energy storage is initiated by a charge separation event [1]. This transfer process has been studied using classical Förster theory or a (modified) Redfield/Lindblad description [2, 3, 4, 5, 6, 7, 8, 9, 10]. Several measures such as the energy transfer efficiency/quantum yield, transfer time, and exciton lifetime have been employed to elucidate the performance of exciton transfer [11, 12, 13]. Recent experiments suggest evidence of long-lived quantum coherence in the Fenna-Matthews-Olson (FMO) protein complex of the Green-Sulphur bacterium *Chlorobium tepidum* and in the reaction center of the purple bacterium *Rhodobacter sphaeroides* [14, 15]. A naturally arising question is the role of coherence in the biological function of the aforementioned chromophoric complexes.

In this work, we investigate relevant quantum coherence effects by an *in-situ* analysis of a success criterion for the initial step in photosynthesis, the energy transfer efficiency (ETE). The dynamics of an excitation in multi-chromophoric complexes can be described in terms of an environment-assisted quantum walk [10]:

$$\frac{d}{dt}\rho(t) = \mathcal{M}\rho(t). \qquad (1)$$

The evolution generated by the superoperator $\mathcal{M}$ connects the population and coherence elements of the density matrix ρ. We assume in this paper that $\mathcal{M}$ is time-independent. We would like to explore and characterize the dynamics of Eq. (1), especially the role of quantum coherence, the environment, and spatial energy transfer pathways. For closely packed multichromophoric arrays, such as the FMO complex, one has to account for strong inter-molecular coupling and quantum coherence effects. A classical approximation of the master equation would be an insufficient description of the open quantum dynamics. Specifically, we want to avoid any comparison of the actual open quantum system under study with a fictitious or abstract model system, such as a high temperature limit, a strong decoherence model, or a semi-classical Förster method.

This is in contrast to studies e.g. in the area of quantum information that compare the quantum dynamics to classical dynamics, for example in the case of the comparison of a classical random walk to a quantum walk [16].

We quantify the role of the various physical processes involved in the energy transfer process in terms of their contribution to the ETE. Formally, we will partition the overall ETE, η, into a sum of terms,

$$\eta = \sum_k \eta_k, \qquad (2)$$

corresponding to a physical decomposition $\mathcal{M} = \sum_k \mathcal{M}_k$. Each term η_k can be interpreted as a contribution to the overall efficiency originating from a particular process $\mathcal{M}_k$. For example, we will split the superoperator into the major components describing the exciton dynamics: coherent evolution with the excitonic Hamiltonian, relaxation within the single-exciton manifold, and dephasing. The η_k associated with the coherent part will then give an indication of the role of quantum evolution to the energy transfer efficiency and hence to the biological function within a particular chromophoric complex. We note that the exact partitioning of the ETE into a sum of terms like Eq. (2) is a non-trivial task: as will be described below, the ETE essentially involves an exponential mapping of the complete superoperator $\mathcal{M}$. A separation of the ETE into a *product* of terms would seem more natural but would not allow the interpretation of η_k as contributions.

In the following sections, we briefly discuss the structure of the superoperator $\mathcal{M}$ and introduce two complementary measures of efficiency contributions: one is based on a Green's function method and the other is derived from energy transfer susceptibilities. We apply these two approaches to the study of the ETE in the FMO complex. We employ a standard Redfield model with the secular approximation which leads to a master equation in Lindblad form [19]. This model captures major decoherence effects such as relaxation and dephasing. We also include spatial correlation of the fluctuations. The Markovian approximation neglects temporal correlations in the phonon bath which can be relevant in photosynthetic systems and will be treated in subsequent work. We believe that this model and our methods can provide insight into the role of quantum coherence in energy transfer, a process that occurs in noisy, ambient temperature environments.

II. MASTER EQUATION FOR MULTICHROMOPHORIC SYSTEMS

The transport dynamics of a single excitation is described by a master equation for the density matrix that includes coherent evolution, relaxation, and dephasing. Moreover, the exciton can recombine or be trapped. The Hamiltonian for an interacting N-chromophoric system in the presence of a single excitation can be written as [8]:

$$H_{\mathrm{S}} = \sum_{m=1}^{N} \epsilon_m |m\rangle\langle m| + \sum_{n<m}^{N} V_{mn}(|m\rangle\langle n| + |n\rangle\langle m|), \quad (3)$$

where the Hilbert space basis states $|m\rangle$ denote the presence of an excitation at the mth chromophore and ϵ_m are relative site energies with respect to the chromophore with the lowest absorption energy. The V_{mn} can be due to Coulomb coupling of the transition densities (Förster) or due to overlap of electronic wavefunctions (Dexter). We denote the eigenbasis of the Hamiltonian (3) as the exciton basis $|M\rangle = \sum_m c_m(M)|m\rangle$, where $H_{\mathrm{S}}|M\rangle = \epsilon_{\mathrm{M}}|M\rangle$. The multichromophoric system interacts with a thermal phonon bath. The dominant component of the system-bath Hamiltonian is associated with site-energy fluctuations [17, 18], i.e. $H_{\mathrm{SB}} = \sum_m q_m |m\rangle\langle m|$, where q_m are operators describing the coupling to the coordinates of the harmonic-oscillator bath. The phonon terms $q_m |m\rangle\langle m|$ induce relaxation and dephasing without changing the number of excitations. We assume that the bath correlator can be simplified as $\langle q_m(t)q_n(0)\rangle = C_{mn}\langle q(t)q(0)\rangle$. C_{mn} is a dimensionless time-independent factor that takes into account the spatial correlations in the phonon bath. For spatially uncorrelated environments it will simply be given by $C_{mn} = \delta_{mn}$. In this work, we will also take into account a phenomenological model for these correlations as will be explained later. The time-dependent part of the correlator is the same for all sites [17]. Additionally, there are two processes that lead to irreversible loss of the exciton [10, 11, 12, 13]. One is the excitation loss due to recombination of the electron-hole pair. The other mechanism describes the excitation transfer to the reaction center (acceptor) and subsequent trapping associated with the charge separation event. These effects are taken into account by the anti-Hermitian Hamiltonians, $-\mathrm{i}H_{\mathrm{recomb}} = -\mathrm{i}\hbar\Gamma\sum_m^N |m\rangle\langle m|$, with Γ the inverse lifetime of the exciton and $-\mathrm{i}H_{\mathrm{trap}} = -\mathrm{i}\hbar\sum_m^N \kappa_m |m\rangle\langle m|$, with κ_m the trapping rates at site m.

In summary, the dynamics of the reduced density matrix of the system can be described by the Lindblad master equation in the Born-Markov and secular approximations as [19]:

$$\frac{d\rho(t)}{dt} = -\frac{\mathrm{i}}{\hbar}[H_{\mathrm{S}} + H_{\mathrm{LS}}, \rho(t)] + \mathcal{L}\rho(t) \quad (4)$$
$$-\frac{1}{\hbar}\{H_{\mathrm{recomb}}, \rho(t)\} - \frac{1}{\hbar}\{H_{\mathrm{trap}}, \rho(t)\},$$

where $\{,\}$ denotes the anti-commutator. The right-hand side of Eq. (4) defines the superoperator $\mathcal{M}$. $\mathcal{L}$ is the Lindblad superoperator derived from the phonon bath coupling,

$$\mathcal{L}\rho(t) = \sum_{\omega,m,n} \gamma_{mn}(\omega)[A_m(\omega)\rho(t)A_n^\dagger(\omega) \quad (5)$$

$$-\frac{1}{2}A_m(\omega)A_n^\dagger(\omega)\rho(t) - \frac{1}{2}\rho(t)A_m(\omega)A_n^\dagger(\omega)].$$

The sum runs over all possible transitions in the single exciton manifold and all the sites. The Lindblad generators are $A_m(\omega) = \sum_{\epsilon_{\mathrm{M}} - \epsilon_{\mathrm{N}} = \hbar\omega} c_m^*(M)c_m(N)|M\rangle\langle N|$, where the summation runs over all transitions with frequency ω in the single-excitation manifold. The Fourier transform of the bath correlation function leads to the rates $\gamma_{mn}(\omega) = 2\pi C_{mn}[J(\omega)(1 + n(\omega)) + J(-\omega)n(-\omega)]$, where $n(\omega)$ is the bosonic distribution function at temperature T. Here, we assume an Ohmic spectral density with $J(\omega) = 0$ for $\omega < 0$ and $J(\omega) = \frac{E_{\mathrm{R}}}{\hbar\omega_c}\omega\exp(-\frac{\omega}{\omega_c})$ elsewhere, with cutoff ω_c, and reorganization energy $E_{\mathrm{R}} = \hbar\int_0^\infty d\omega\frac{J(\omega)}{\omega}$ [17]. The pure dephasing part of Eq. (5) is obtained in the limit $\omega \to 0$. The Lindblad generators are $A_m(0) = \sum_M |c_m(M)|^2 |M\rangle\langle M|$ and the rate is $\gamma_{\phi,mn} = 2\pi C_{mn}\frac{E_{\mathrm{R}}}{\hbar\omega_c}kT$. The Lamb shift Hamiltonian [19] is given by $H_{\mathrm{LS}} = E_{\mathrm{R}}\sum_{M,m}|c_m(M)|^4 |M\rangle\langle M|$, where we only take into account the most significant, diagonal part, see Ref. [18] and supplementary material thereof.

The competition of trapping and recombination processes leads to the concept of the energy transfer efficiency (ETE) as the integrated probability of successful exciton entrapment by the reaction center [10, 11, 13],

$$\eta = \frac{2}{\hbar}\int_0^\infty \mathrm{Tr}\{H_{\mathrm{trap}}\rho(t)\}dt. \quad (6)$$

The efficiency is suppressed by the lifetime of the excitation due to exciton recombination. Quantitatively, the suppression is given by the "deficiency", $\bar\eta = \frac{2}{\hbar}\int_0^\infty \mathrm{Tr}\{H_{\mathrm{recomb}}\rho(t)\}dt$. One finds the relation $\eta + \bar\eta = 1$ which implies that the excitation ultimately either is trapped or recombines.

III. CONTRIBUTIONS TO THE ENERGY TRANSFER EFFICIENCY

We partition the efficiency based on a Green's function method. First, note that with Eq. (1) the efficiency can be simplified as

$$\eta = -\frac{2}{\hbar}\mathrm{Tr}\{H_{\mathrm{trap}}\mathcal{M}^{-1}\rho(0)\}, \quad (7)$$

The trapping and recombination Hamiltonians ensure that $\mathcal{M}$ is invertible since non-trivial eigenstates with zero eigenvalue, such as the usual thermal equilibrium, do not exist. The Green's function interpretation of $-\mathcal{M}^{-1}$ can be readily confirmed by examining the Laplace-transformed master equation. Next, the superoperator is decomposed into $\mathcal{M} = \mathcal{H}_{\mathrm{ref}} + \mathcal{R}$, where the recombination-trapping part $\mathcal{H}_{\mathrm{ref}}\rho = -\frac{1}{\hbar}\{H_{\mathrm{recomb}}, \rho(t)\} - \frac{1}{\hbar}\{H_{\mathrm{trap}}, \rho(t)\}$, is taken as a reference point and the remainder is given by $\mathcal{R}\rho = -\frac{\mathrm{i}}{\hbar}[H_{\mathrm{S}} + H_{\mathrm{LS}}, \rho] + \mathcal{L}\rho$. This allows us to express the Green's function exactly as [20],

$$\mathcal{M}^{-1} = \mathcal{H}_{\mathrm{ref}}^{-1} + \mathcal{H}_{\mathrm{ref}}^{-1}\mathcal{R}\mathcal{M}^{-1}. \quad (8)$$

The first term in (8) describes the irreversible dynamics resulting from excitonic transfer to the acceptor and recombination of the excitation. The second term accounts for the effect of the Hamiltonian and the Lindblad operator. This term can be decomposed into various physical processes such as coherent hopping or phonon-mediated jumps from site-to-site, $\mathcal{R} = \sum_k \mathcal{R}_k$. We use Eq. (8) and the relation $\eta = 1 - \bar{\eta}$ to arrive at the partitioning of the efficiency, $\eta = \sum_k \eta_k$, with

$$\eta_k = -\frac{2}{\hbar}\mathrm{Tr}\{H_{\mathrm{recomb}}\mathcal{H}_{\mathrm{ref}}^{-1}\mathcal{R}_k\mathcal{M}^{-1}\rho(0)\}. \qquad (9)$$

The part related to the first term in Eq. (8) gives just one and thus cancels with the one from the conservation property. Note that each η_k is dependent on the initial state, the overall dynamics $\mathcal{M}^{-1}$, and the particular process $\mathcal{R}_k$ weighted by a diagonal trapping-recombination operator $H_{\mathrm{recomb}}\mathcal{H}_{\mathrm{ref}}^{-1}$. The trace then takes into account the local effect of $\mathcal{R}_k$ on the population of all the site basis states $|m\rangle$.

IV. APPLICATION TO THE FMO COMPLEX

The Fenna-Matthews-Olson protein complex is a chromophoric trimer where each subunit consists of seven chlorophylls embedded in a protein environment [14, 21, 22]. It connects the photosynthetic antenna with the reaction center in *Chlorobium tepidum*. We use the seven-level Hamiltonian of the FMO complex as given in Ref. [17] and the bath spectrum described earlier with the reorganization energy $E_{\mathrm{R}} = 35\mathrm{cm}^{-1}$ and cutoff $\omega_c = 150\mathrm{cm}^{-1}$, inferred from Fig. 2 of Ref. [18]. The transfer of the excitation from the FMO to the reaction center occurs via site 3 with the rate κ_3, which is a free parameter in our simulations and, if not otherwise stated, is taken to be $\kappa_3 = 1\mathrm{ps}^{-1}$ [10]. The exciton lifetime is assumed to be $1/\Gamma = 1\mathrm{ns}$ [23]. The initial state for the simulation is taken to be an unbiased classical mixture of all sites except the trapping site 3. At first, we will assume that the phonon modes at different chlorophylls are not spatially correlated with each other, which is equivalent to setting $C_{mn} = \delta_{mn}$. Later, we will relax this assumption and investigate the contributions as a function of a phenomenological parameter, the correlation length R_c.

In Fig. 1 (left panels) we present the contributions to the ETE as a function of three relevant system parameters for the three fundamental physical processes: Hamiltonian evolution with H_{S} and exciton relaxation and dephasing, both contained in $\mathcal{L}$. The parameters explored are the reorganization energy E_{R}, which is a linear prefactor of all the decoherence rates, the transfer rate to the reaction center κ_3, and temperature T. In Ref. [10], we reported the overall behavior of the efficiency with respect to these parameters, especially the enhancement of the ETE by about 20% compared to no phonon-bath, $E_{\mathrm{R}} = 0$. Even more significantly, the transport time of the excitation to the reaction center reduces from over 50ps to under 5ps. Here, by providing a more detailed analysis of the underlying processes, we observe a crossover from a purely quantum regime to a relaxation-dominated regime with increasing phonon bath coupling strength E_{R}, see Fig. 1 (a).

At room temperature and $E_{\mathrm{R}} = 35\mathrm{cm}^{-1}$ the purely quantum mechanical contribution of coherent hopping due to the Hamiltonian is around 10%. This is the main result of this work and is to be understood within the context of our model and its approximations. The major contribution is due to exciton relaxation induced by the phonon-bath coupling. Site 3 has a large participation in the lowest-energy exciton: relaxation helps the transport from the energetically higher initial state towards that site. Dephasing processes have a contribution of around 8% (see explanation below). To summarize, the results so far indicate that the process of energy relaxation determines the high efficiency and the fast transfer times f the Fenna-Matthews-Olson protein complex and thus is essential to the biological function of this system. Supporting this statement is a recent study that finds that the protein environment induces a static red-shift of the energy of site 3 [22].

Slow movement of the protein scaffold will lead to static disorder in the Hamiltonian and thus to inhomogeneous broadening of spectral lines. We obtain the effect of static disorder on the efficiency and the contributions by averaging over diagonal disorder of the site energies ϵ_m. We assume that the site energies are normal distributed around the Hamiltonian given in [17] and with a site-dependent FWHM σ_m. Based on the supplementary material of Ref. [22] we choose $\sigma_{1,3,4} = 60\mathrm{cm}^{-1}$, $\sigma_2 = 100\mathrm{cm}^{-1}$, and $\sigma_{5,6,7} = 120\mathrm{cm}^{-1}$. These values lead to good agreement of measured and simulated spectra and can be explained by the different amounts of mobile water molecules in the vicinity of the different chlorophylls of the FMO protein complex. In Fig. 1 the resulting distributions of the efficiency and the contributions are depicted as error bars. At small E_{R} the efficiency and the prevalent quantum mechanical contribution have a broadening of around 10%. This is due to the fact that the static disorder changes the energy difference of interacting sites which can facilitate or inhibit transport. At larger E_{R} the efficiency has a small broadening of less than 1%. In the presence of an environment the system is more robust against static disorder. A smaller contribution of the quantum mechanical part is compensated by a larger contribution of relaxation and vice versa.

Fig. 1 (b) shows the dependence of the contributions on the transfer rate to the acceptor. The behavior can be explained by the characteristic time scales of the various processes. At room temperature and $E_{\mathrm{R}} = 35\mathrm{cm}^{-1}$, the relaxation processes occur on a time scale of 1ps and are most important when the acceptor rate is of the same order of magnitude. The Hamiltonian and dephasing act on faster time scales such that their contributions are stronger at higher acceptor rate values. The contribution of dephasing can be understood from the fact that, within the Redfield/Lindblad treatment, dephasing acts in the energy basis: an initial state localized at a site dephases to a state that has overlap with the target site. For example, the initial state $\rho(0) = |1\rangle\langle 1| = \sum_{M,N} c_1(M)c_1^*(N)|M\rangle\langle N|$ evolves in the presence of only dephasing to $\rho(t \to \infty) = \sum_M |c_1(M)|^2|M\rangle\langle M|$, which has $\langle 3|\rho(t \to \infty)|3\rangle \neq 0$.

Finally, Fig. 1 (c) shows the temperature dependence of the ETE contributions at $E_{\mathrm{R}} = 35\mathrm{cm}^{-1}$. The role of the Hamiltonian is about 20% at zero temperature. The relaxation processes are only weakly dependent on T: the main contribu-
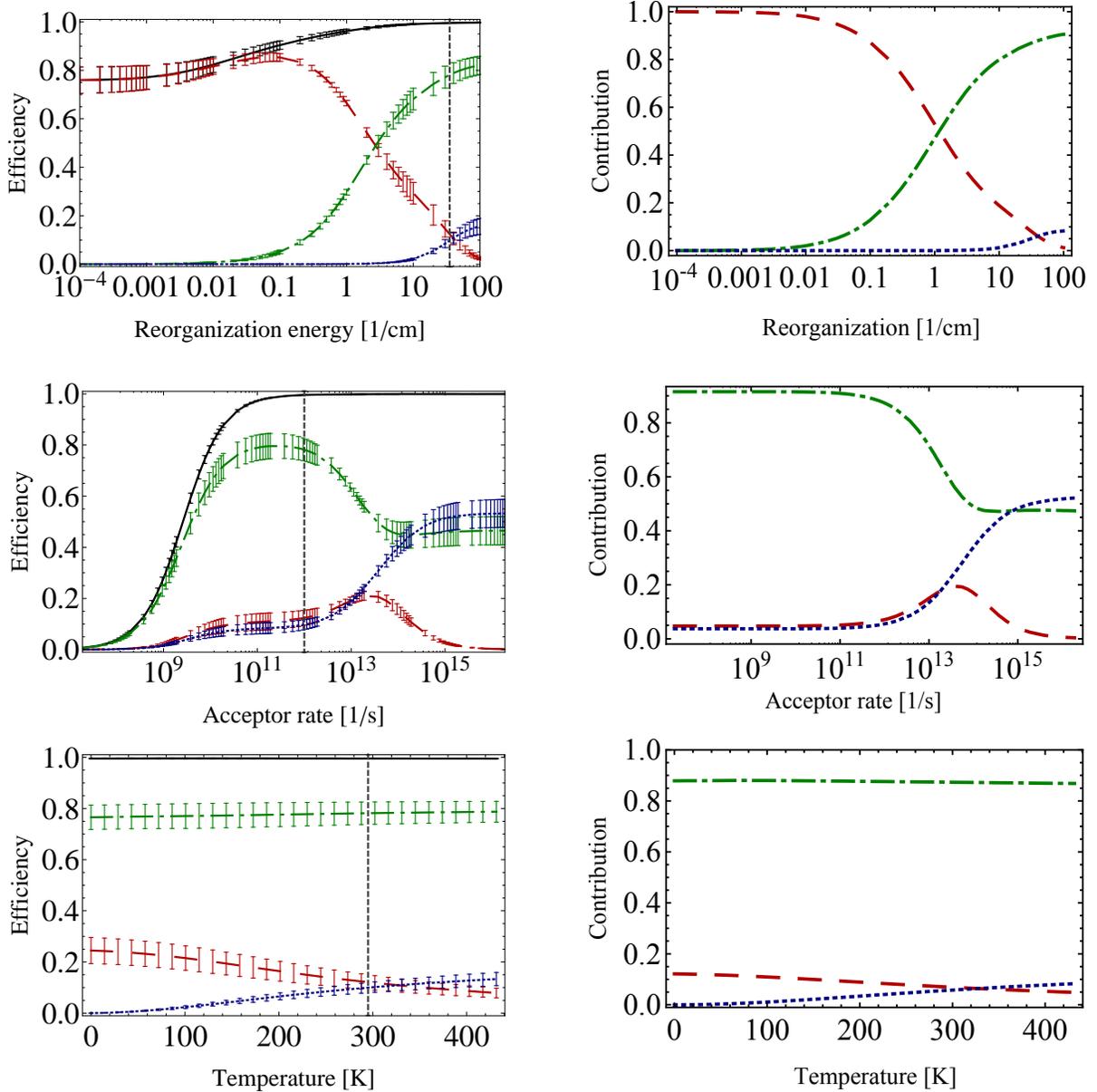
FIG. 1: Contributions of the basic physical processes to the overall energy transfer efficiency of the Fenna-Mathews-Olson protein complex according to Eq. (9) (left panels) and Eq. (11) with normalization (12) (right panels). The physical processes are the Hamiltonian evolution (red, − −), exciton relaxation (green, − ·), and exciton dephasing (blue, · · ·). They add up to the efficiency (black, −) (left) or 1 (right). Depicted are the contributions as a function of a) reorganization energy, essentially the overall strength of the phonon-bath coupling b) the transfer rate to the reaction center, and c) the temperature. We assume that the initial state is an unbiased classical mixture of all the sites of the FMO complex except target site 3. Typical parameters (shown as vertical lines) are $E_R = 35 \text{cm}^{-1}$, $T = 295$K, $\kappa_3 = 1\text{ps}^{-1}$, and $\Gamma = 1\text{ns}^{-1}$ [18]. Using these parameters, the first (second) measure on the left (right) gives an estimated contribution of 80% (87.5%) for exciton relaxation and 10% (7.5%) for the Hamiltonian evolution at room temperature.

tion is the temperature-independent spontaneous emission of energy into the phonon bath, leading to energy funneling towards the site with the lowest energy, site 3. The behavior of the dephasing processes is explained by $\gamma_\phi \sim kT$. In all figures, the contribution of the Lamb shift Hamiltonian is less than 1.5% and thus not depicted.

Up to this point we assumed that the site energy fluctuations

of a particular site caused by the coupling to a vibrational bath are uncorrelated from the fluctuations at another site. We relax this assumption to take into account spatially correlated fluctuations present in realistic chromophoric systems embedded in a protein environment. Specifically, instead of an uncorrelated environment with $C_{mn} = \delta_{mn}$ we include correlations with $C_{mn} = e^{-R_{mn}/R_c}$ [18]. R_{mn} is the intermolecular dis-
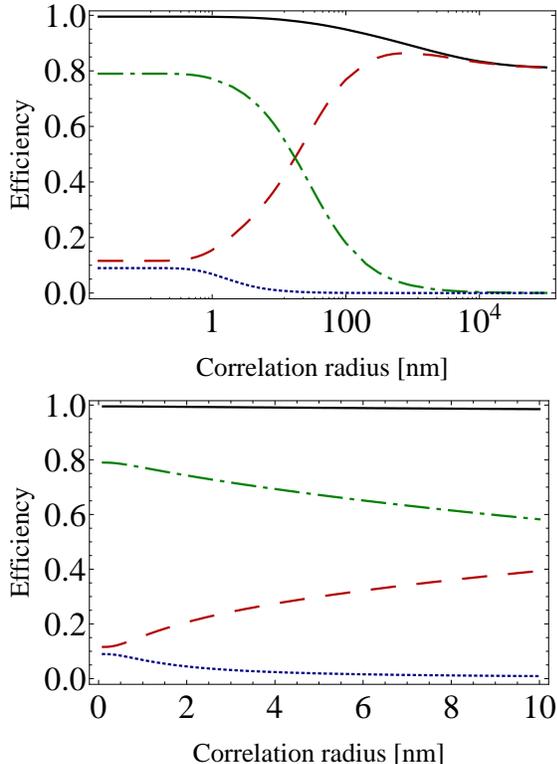
FIG. 2: Efficiency and contributions of the basis physical processes as a function of the correlation radius in the environment in the Fenna-Matthews-Olson complex. The parameters used are $E_R = 35 \text{cm}^{-1}$, $T = 295\text{K}$, $\kappa_3 = 1\text{ps}^{-1}$, and $\Gamma = 1\text{ns}^{-1}$. The lower panel is a magnification of the physically relevant region of the upper panel.

tance between chlorophyll m and n and R_c is the correlation radius. In the limit of $R_c \rightarrow 0$ one has the uncorrelated case. In the limit of $R_c \rightarrow \infty$ all fluctuations are perfectly correlated and thus lead only to an irrelevant global phase in the exciton dynamics: this limit is equivalent to no phonon bath at all. In Fig. 2 we plot the efficiency and the contributions as a function of the correlation radius for the Fenna-Matthews-Olson protein complex. We recover the two limits: at small correlation radius the efficiency and the contributions are the same as in Fig. 1. For large correlation radius the quantum coherence contribution is dominant and there is no contribution of relaxation and dephasing. In between, we observe a crossover which happens when the correlation radius is of the order of the intermolecular distance.

V. BEYOND LOCAL CONTRIBUTIONS

The method for partitioning the efficiency into contributions presented in the last section sheds light on the role of the basic physical processes in the overall open systems dynamics. Our approach resembles the sojourn expansion used in Ref. [11] for a classical random walk and the method used

in Ref. [12] for studying incoherent versus coherent energy transfer in the Haken-Strobl model. However, it shows a certain local feature: only processes that are directly connected to site population elements play a role. This can be seen in Eq. (9) from the fact that $\mathcal{H}_{\text{ref}}^{-1}$ and H_{recomb} are diagonal operators. Thus the contributions of all $\mathcal{R}_k$ which do not lead to transfer to a site population vanish in the trace, e.g., in the case of coherence to coherence processes. Note that this effect would have been pronounced had we not used the identity $\eta = 1 - \bar{\eta}$ before Eq. (9). In this case only those $\mathcal{R}_k$ that create overlap with the target site 3 would contribute. To overcome these issues, we develop our complementary measure motivated by the concept of energy transfer susceptibilities, discussed in [10].

In this method, we partition the efficiency into terms involving the variational change of the excitation trapping probability density $\frac{2}{\hbar}\text{Tr}\{H_{\text{trap}}\rho(t)\}$ with respect to the different physical processes. We first provide a representation for a quantum master equation in the Markov approximation that is tailored to the problem at hand:

$$\frac{d}{dt}\rho(t) = \sum_k \frac{1}{t} \int_0^t \mathcal{F}(t, t') \mathcal{M}_k \mathcal{F}(t', 0) \rho(0) dt'. \quad (10)$$

We used the decomposition $\mathcal{M} = \sum_k \mathcal{M}_k$ and the quantum map $\rho(t) = \mathcal{F}(t, 0)\rho(0)$. This equation is equivalent to Eq. (1), but the individual terms in the sum are different from just $\mathcal{M}_k$: the integrand can be understood as the realization of a non-unitary quantum walk in Liouville space. The quantum walk starts at the initial state $\rho(0)$, evolves with $\mathcal{F}$ for a time interval of $[0, t']$, then a perturbation $\mathcal{M}_k$ is applied at an arbitrary time t', after which it undergoes a post-evolution until time t. The second evolution $\mathcal{F}(t, t')$ leads to quantum interference between $\mathcal{M}_k$ and other generators. Integrating over all possible paths gives the average effect of the kth generator to the time variation of the density matrix.

Eq. (10) can be reexpressed by introducing scalar dimensionless quantities λ_k associated with each term $\mathcal{M}_k$, such that $\mathcal{M}_k \rightarrow \lambda_k \mathcal{M}_k$ in the neighborhood $\lambda_k \rightarrow 1$. This leads to the master equation $\frac{d}{dt}\rho(t) = \frac{1}{t}\sum_k \frac{\partial}{\partial \lambda_k}\rho(t)$, which is equivalent to Eq. (10). We employ it to partition the ETE in Eq. (6) into contributions given by

$$\eta_k = \frac{2}{\hbar} \int_0^\infty dt \int_0^t dt' \frac{1}{t'} \frac{\partial}{\partial \lambda_k} \text{Tr}\{H_{\text{trap}}\rho(t')\}. \quad (11)$$

We assume that the initial state $\rho(0)$ has no overlap with the trapping sites. The terms $\frac{2}{\hbar}\frac{\partial}{\partial \lambda_k}\text{Tr}\{H_{\text{trap}}\rho(t)\}$ can be interpreted as the susceptibility with respect to the process $\mathcal{M}_k$ of the exciton trapping probability density $\frac{2}{\hbar}\text{Tr}\{H_{\text{trap}}\rho(t)\}$ at time t. The double integration is then to be considered as a time averaging of this quantity. The factor $\frac{1}{t}$ in the integrand arises from Eq. (10). We solve Eq. (11) by numerical integration. The resulting contributions η_k are not normalized, meaning that $0 \leq \eta_k \leq 1$ does not necessarily hold. To define a proper normalization we separate the η_k into positive and negative terms, i.e. $\eta = \eta^+ + \eta^- = \sum_{k_+} \eta_{k_+} + \sum_{k_-} \eta_{k_-}$ where one has $\eta_{k_+} > 0$ and $\eta_{k_-} < 0$ and the overall positive or negative contributions $\eta^{\pm}$. Now one can introduce a
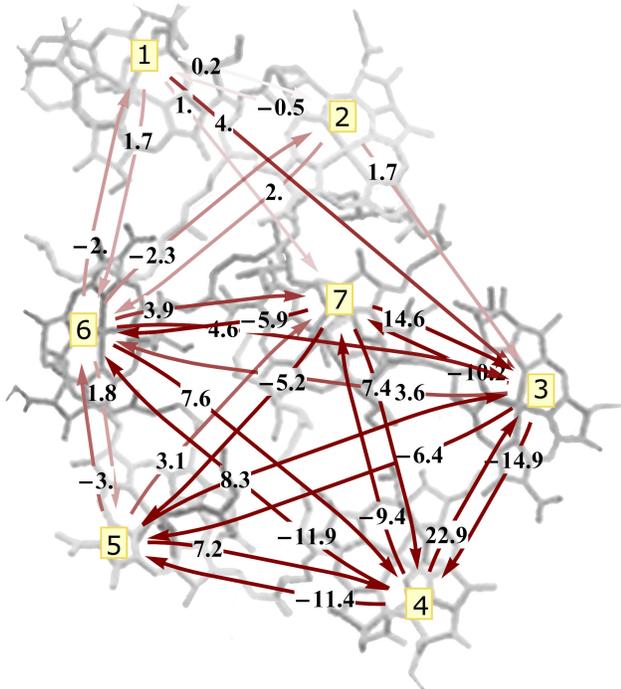
FIG. 3: The Fenna-Matthews-Olson protein complex and the contributions in percent of the relaxation pathways to the overall relaxation contribution of the energy transfer efficiency, using Eq. 11 and the normalization Eq. 12. For clarity some contributions below 2% are not depicted. The initial state is a classical mixture of all sites except target site 3. Standard parameters are $E_{\rm R} = 35{\rm cm}^{-1}$, $T = 295$K, $\kappa_3 = 1{\rm ps}^{-1}$, and $\Gamma = 1{\rm ns}^{-1}$. The contributions show directionality in their sign and reveal the important pathways.

normalization given by:

$$\widetilde{\eta}_{k_{\pm}} = \frac{\eta_{k_{\pm}}}{\eta^{\pm}}. \qquad (12)$$

This allows us to interpret $\widetilde{\eta}_{k_{\pm}}$ as positive or negative percentage contributions to the overall positive or negative contribution. The normalized contributions $\widetilde{\eta}_{k_{\pm}}$ show similar behavior for the basic processes as the Green's function measure Eq. (9), see Fig. 1 (right panels). This can be seen as evidence that, one the one hand, the normalization procedure was appropriate and, on the other hand, that despite its local feature the Green's function measure obtains consistent results. The second measure generally assigns less contribution to the free Hamiltonian, about 7.5% at $E_{\rm R} = 35{\rm cm}^{-1}$

and $T = 295K$. For these parameters, the contribution of relaxation is about 87.5% and dephasing about 5%. At zero temperature the Hamiltonian contribution is 12.5%.

The measure based on susceptibilities can be used to quantify the contributions of exciton relaxation pathways in the site basis. Formally, we look at the contribution of all site-to-site jumps and the corresponding damping of diagonal populations, see Ref. [10]. In Fig. 3 we show the contributions of the various pathways for the Fenna-Matthews-Olson protein complex when the system is initially in a classical mixture of all sites except the target site 3. Jumps toward the target site 3 contribute positively while jumps away from the target site contribute negatively. Large contributions come from nearest neighbor jumps, and site 4 and 7 are revealed as hubs in the transfer toward site 3.

VI. CONCLUSION

In this work, we have addressed the role of quantum coherence and the environment in excitonic energy transfer. To this end, we have characterized the underlying processes constituting the open quantum walk of the excitation in terms of their contribution to the transfer efficiency. The methods presented here are general and can be applied to a large class of transport systems in the presence of Markovian environments. Within both the Green's function and the energy transfer susceptibility formalisms we conclude that the major part of the high efficiency of the Fenna-Matthews-Olson protein complex of about 80% or 87.5% is due to environment-induced relaxation down to the lowest energy site. The role of quantum coherence induced by the Hamiltonian dynamics can be quantified at around 10% or 7.5% respectively. Furthermore, we used the susceptibility measure to assign percentage-wise contributions to exciton relaxation pathways in the molecular basis. The detailed analysis of the open quantum dynamics presented in this work could be harnessed for engineering artificial materials such as quantum dots [25] to achieve optimal energy transport in realistic environments.

[1] R.E. Blankenship, *Molecular Mechanism of Photosynthesis* (Blackwell Science, London, 2002).

[2] T. Förster, in *Modern Quantum Chemistry, Istanbul Lectures*, edited by O. Sinanoglu (Academic, New York, 1965), Vol. 3, pp. 93–137.

[3] M. Grover and R. Silbey, J. Chem. Phys. **54**, 4843 (1971).

[4] X. Hu, T. Ritz, A. Damjanović, K. J. Schulten, Phys. Chem. B, **101**, 3854 (1997).

[5] M. Yang and G. R. Fleming, Chem Phys **275**, 355 (2002).

[6] G. D. Scholes, Annu. Rev. Phys. Chem. 54 , 57-87 (2003).

[7] V. I. Novoderezhkin, M. A. Palacios, H. van Amerongen, R. van Grondelle, J. Phys. Chem. B **108**, 10363 (2004).

[8] V. May and O. Kühn, *Charge and Energy Transfer Dynamics in Molecular Systems* (Wiley-VCH, Weinheim, 2004).

[9] S. Jang, M.D. Newton, and R.J. Silbey, Phys. Rev. Lett. **92**, 218301 (2004).

[10] M. Mohseni, P. Rebentrost, S. Lloyd, A. Aspuru-Guzik, J. Chem. Phys. 129, 174106 (2008).

[11] M.K. Sener, S. Park, D. Lu, A. Damjanović, T. Ritz, P. Fromme, and K. Schulten, J Chem. Phys. **120,** 11183 (2004).

[12] J.A. Leegwater, J. Phys. Chem. **100**, 14403 (1996).

[13] A. Olaya-Castro, C. Fan Lee, F. Fassioli Olsen, and N. F. Johnson, Phys. Rev. B **78**, 085115 (2008).

[14] G.S. Engel, T.R. Calhoun, E.L. Read, T.-K. Ahn, T. Mancal, Y-C. Cheng, R.E. Blankenship, and G.R. Fleming, Nature **446**, 782 (2007).

[15] H. Lee, Y.-C. Cheng, and G.R. Fleming, Science **316**, 1462 (2007).

[16] A. Childs, E. Farhi, and S. Gutmann, Quant. Info. Proc. **1**, 35 (2002).

[17] M. Cho, H.M. Vaswani, T. Brixner, J. Stenger, and G.R. Fleming, J. Phys. Chem. B **109,** 10542 (2005).

[18] J. Adolphs and T. Renger, Biophys. J. **91,** 2778 (2006).

[19] H. -P. Breuer and F. Petruccione, *The Theory of Open Quantum Systems* (Oxford University Press, New York, 2002).

[20] S. Mukamel, *Principles of Nonlinear Optical Spectroscopy* (Oxford University Press, New York, 1995).

[21] Y. Li, W. Zhou, R. E. Blankenship, and J. P. Allen, J. Mol. Biol. **271,** 456 (1997).

[22] F. Müh, M. El-Amine Madjet, J. Adolphs, A. Abdurahman, B. Rabenstein, H. Ishikita, E.-W. Knapp, and T. Renger, Proc. Natl. Acad. Sci. USA **104**, 16862 (2007).

[23] T.G. Owens, S.P. Webb, L. Mets, R.S. Alberte, and G.R. Fleming, Proc. Natl. Acad. Sci. USA **84**, 1532 (1987).

[24] T. Ritz, S. Park, and K. Schulten, J. Phys. Chem. B **105,** 8259 (2001).

[25] A. Nazir, B.W. Lovett, S.D. Barrett, J.H. Reina, and G.A.D. Briggs, Phys. Rev. B **71**, 045334 (2005).